◀**Fig. 3.4** Impact of bioturbation on gas-reservoir quality based on examples from Upper Cretaceous deep-marine turbidite deposits of the Vøring Basin, Norwegian Sea. **a** Core examples of almost unbioturbated versus intensely bioturbated sandstone and their corresponding porosity and permeability measurements (based on horizontal core plug data), which indicate reduced properties for bioturbated sandstone. Springar Formation (Maastrichtian, well 6604/10-1). **b** Sandstone in thin section with homogeneous texture and incorporated clay minerals, some of which outline the wall of a discrete *Ophiomorpha rudis* burrow. Same well as in (**a**). **c** Callianassid shrimp in its lined burrow similar to *Ophiomorpha*. From Bromley and Asgaard (1972), republished with permission of GEUS. **d** Permeability and porosity cross plot showing the properties of bioturbated versus unbioturbated sandstone, as shown in (**a**) (based on horizontal core plug measurements). The bioturbated sandstone is clearly reduced in porosity and permeability, the latter of which is about one order of magnitude lower than measured for unbioturbated sandstone. **e** Thick unit of turbiditic sandstone with upward-increasing bioturbation (*Ophiomorpha rudis*) towards a sharp bedding surface at its top (ca. 4476.45 m), which goes hand in hand with a reduction of porosity and permeability due to incorporation of mud. The overlying sand unit is unbioturbated and has reasonably high properties. Kvitnos Formation (Santonian, well 6707/10-2A)

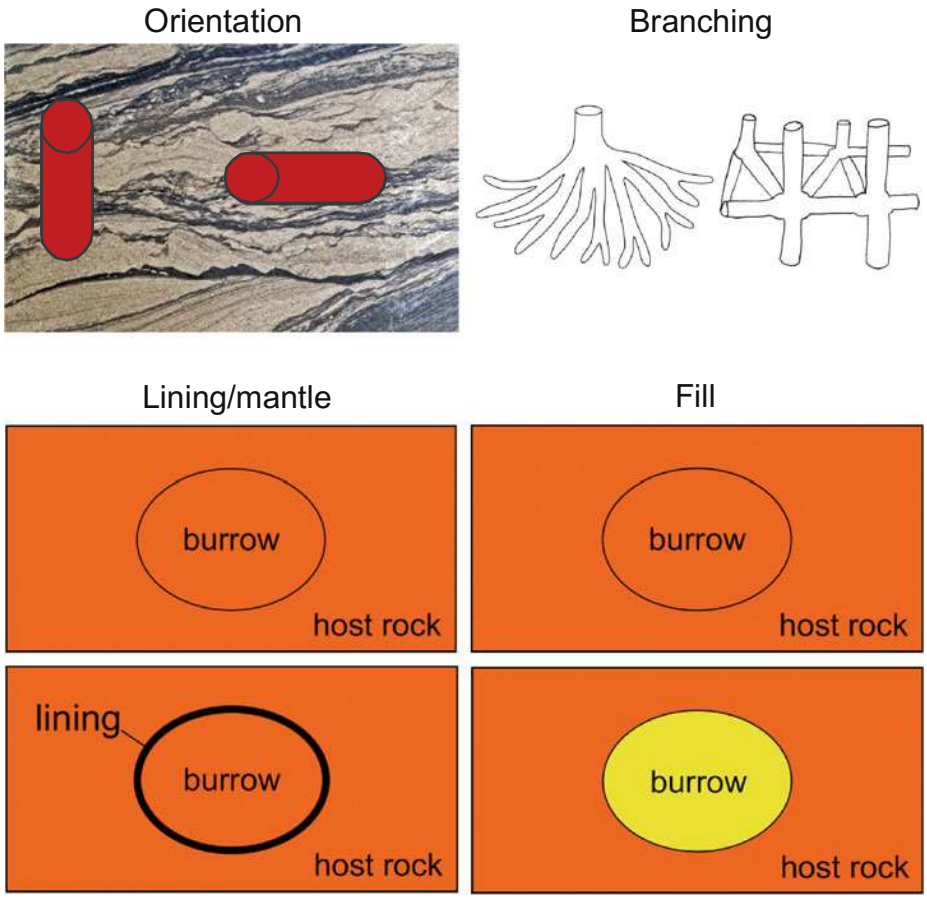


Fig. 3.5 Architectural elements and characteristics of burrows, which may have an impact on reservoir quality, such as burrow orientation with respect to bedding (e.g. horizontal, vertical, oblique), branching (e.g. unbranched, branched, dichotomous, network, boxwork), presence or absence of lining or mantle, and burrow fill (e.g. active, passive) with respect to host rock (e.g. sand, mud). Modified after Knaust (2013)

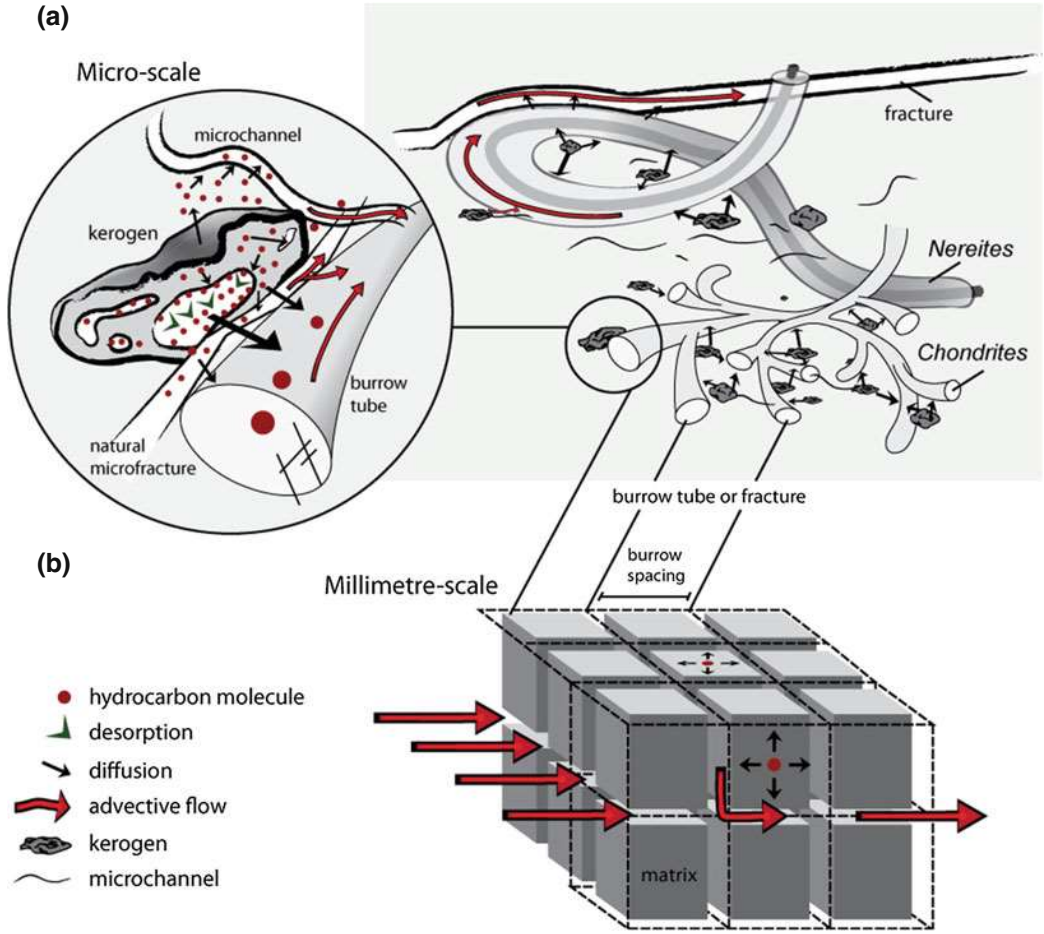


Fig. 3.6 Schematic illustration presenting stages of the fluid flow within bioturbated, gas-charged tight mudstone. From Bednarz and McIlroy (2015), republished with permission of Elsevier; permission conveyed through Copyright Clearance Center, Inc. **a** Micro-scale. As pressure drops, hydrocarbon molecules enter the organo-porosity through desorption from pore walls and kerogen material. If the pore is connected to the (micro-) fracture or micro-channel, molecules travel through the conductive flow paths to the well bore. If there is no fracture or micro-channel connected to the organo-porosity, the molecules travel to the fracture network or permeable flow path through diffusion. **b** Millimetric scale. Efficiency of the flux of the diffusively migrating molecules into the fracture network is dependent on the distance from oil- or gas-charged pore to the closest fracture or permeable flow-path. Dense ichnofabric network minimises the distance of the diffusive flow through partitioning the hosting rock with permeable and brittle silty tubes and may also improve fracture spacing and/or complexity

References

Bednarz M, McIlroy D (2015) Organism–sediment interactions in shale-hydrocarbon reservoir facies—Three-dimensional reconstruction of complex ichnofabric geometries and pore-networks. Int J Coal Geol 150–151:238–251

Bromley RG (1990) Trace fossils: biology and taphonomy. Unwin Hyman, London, 293 pp

Bromley RG, Asgaard U (1972) Notes on Greenland trace fossils, 1. Freshwater *Cruziana* from the Upper Triassic of Jameson Land, East Greenland. Grønlands Geologiske Undersøgelse, Rapport 49: 7–13

Bromley RG, Ekdale AA (1986) Composite ichnofabrics and tiering of burrows. Geol Mag 123:59–65

Knaust D (2013) Bioturbation and reservoir quality: towards a genetic approach. AAPG Search and Discovery Article #50900

Seilacher A (1967) Bathymetry of trace fossils. Mar Geol 5:413–428

Zesshin M, Catuneanu O (2013) High-resolution sequence stratigraphy of clastic shelves I: units and bounding surfaces. Mar Pet Geol 39:1–25